

Modelling random scission of linear polymers

J.E.J. Staggs*

Department of Fuel and Energy, University of Leeds, Leeds LS2 9JT, UK

Received 31 July 2001; received in revised form 1 November 2001; accepted 4 November 2001

Abstract

A mathematical model for the random scission of linear polymers is presented. The model takes the form of a set of ordinary differential equations which describe the evolution of the MW distribution as a function of the fraction of bonds broken. An exact solution, valid for large initial MW, is derived from the equations and compared with results from a Monte-Carlo type simulation. Isothermal thermogravimetric experiments using polyethylene are used to suggest a relationship between the rate of bond breaking and temperature and this is then used to compare model predictions for the rate of degradation with constant heating rate thermogravimetric experiments. Excellent agreement is found between theoretical predictions and experimental results for the case of a standard sample of polyethylene with number-average MW 2015. © 2002 Elsevier Science Ltd. All rights reserved.

Keywords: Random scission; Linear polymer; Polyethylene; Thermal degradation; Mathematical model

1. Introduction

At the heart of modelling ignition and combustion behaviour of solids (as well as other important processes) is a general description of the thermal degradation of the material. For materials such as polymers, four thermal degradation mechanisms are thought to exist, namely random scission, end-chain scission (or unzipping), chain stripping and cross linking [1]. Traditional descriptions of these mechanisms have relied on applying one or more kinetic rate equations of the form

$$\frac{d\mu}{dt} = -\mu^v \kappa(T), \quad (1)$$

where μ is the mass fraction of a particular component, v is the reaction order and κ is usually assumed to be of Arrhenius form $\kappa(T) = A \exp(-T_A/T)$ [2,3]. Note that T_A is also sometimes written in terms of an activation energy E_A , as $T_A = E_A/R$, where R is the gas constant. This approach essentially borrows ideas from statistical mechanics and the description of reactions between gas particles [4] and attempts to apply them to the degradation of solids with little or even no theoretical

justification. Having stated this, it is proper to redress the balance a little and record the fact that these descriptions often do reproduce experimental data such as thermogravimetric analyses well. For example, the work of Bockhorn and collaborators [5–7] has produced good results for a number of polymers.

For the case of random scission, alternative models, which are sounder in theory, exist. For example, Emsley and Heywood [8] used a numerical Monte-Carlo type simulation to investigate degradation of linear polymers where a number of bond-breaking regimes were investigated. Platowski and Reichert [9], again using Monte Carlo methods, investigated modelling the kinetics of polymerisation reactions (the reverse process of the present subject admittedly, but still relevant in concept). Other more involved treatments include molecular dynamics simulations for depolymerisation of simple polymers [10–12] and the recent contribution of Doruker et al., [13] for the random scission of C–C bonds in polyethylene.

The present work extends the approach of Emsley and Heywood [8]. A mathematical model is developed in the form of a set of ordinary differential equations describing the evolution of the MW distribution for a linear polymer undergoing scission by a random process. An exact solution is derived and then used to compare predictions with Monte Carlo type simulations and thermogravimetric experiments using polyethylene.

* Tel.: +44 (0) 113 233 2495; fax: +44 (0) 113 244 0572.

E-mail address: j.e.j.staggs@leeds.ac.uk

Nomenclature

f_m	Relative frequency
k	Rate of bond breaking/s ⁻¹
\bar{m}	Average size of molecule in distribution
m_v	Threshold molecular size for volatile products
n	Initial number of repeat units in molecule
r	Fraction of bonds broken in distribution
t	Time/s
A	Pre-exponential factor/s ⁻¹
B	Number of unbroken bonds in distribution
H	Heating rate/K s ⁻¹
E_1	The exponential integral $E_1(z) = \int_z^\infty e^{-t}/t dt$
N	Number of molecules in distribution
N_m	Number of molecules in distribution with m repeat units
T	Temperature/K
T_A	Activation temperature/K
μ	Ratio of sample mass to initial mass
χ	Degree of polymerisation

1.1. General concepts and definitions

For the purposes of the mathematical model, the polymer molecule will be viewed as consisting of a linear chain of repeat units linked by bonds which may break during the degradation process. Consider a large number $N(r)$ of these idealised molecules initially consisting of n repeat units and $n-1$ bonds between repeat units, where r is the fraction of bonds broken at any stage. Let $N_m(r)$ denote the number of molecules in the distribution with m repeat units and let $f_m(r)$ be the corresponding relative frequency, i.e. $f_m(r) = N_m(r)/N(r)$. Thus the total number of unbroken bonds $B(r)$ in the distribution will be $B(r) = \sum_{m=1}^n (m-1)N_m(r)$ and r is given implicitly by $r = 1 - B(r)/B(0)$. Now, defining $\bar{m}(r)$ in an analogous fashion to the number-average molecular weight, i.e. $\bar{m}(r) = \sum_{m=1}^n m f_m(r)$, it follows that $B(r) = N(r)(\bar{m}(r) - 1)$ and so we can write

$$1 - r = \frac{N(r)(\bar{m}(r) - 1)}{N(0)(\bar{m}(0) - 1)}. \quad (2)$$

Now since each time a bond is broken the total number of molecules in the distribution increases by 1, so it follows that N increases linearly with r according to $N(r) = N(0) + rB(0)$, and so

$$\frac{N(r)}{N(0)} = 1 + r(\bar{m}(0) - 1). \quad (3)$$

Using this last relation with (2) gives

$$\bar{m}(r) = \frac{\bar{m}(0)}{1 + r(\bar{m}(0) - 1)}, \quad (4)$$

and we see that, as expected, $N(r)\bar{m}(r) = \text{constant} = N(0)\bar{m}(0)$.

The degree of polymerisation $\chi(r)$ may be defined as the ratio of the initial number of repeat units in the distribution to the number of molecules in the distribution, i.e. $\chi(r) = N(0)\bar{m}(0)/N(r)$. Using Eq. (3) for the ratio $N(r)/N(0)$, it follows that $\chi(r) = \bar{m}(r)$ and so

$$\frac{1}{\chi(r)} - \frac{1}{\chi(0)} = \frac{(\bar{m}(0) - 1)r}{\bar{m}(0)}, \quad (5)$$

i.e. that the reciprocal of the degree of polymerisation is proportional to r . Hence for degradation processes in which $r \propto t$, Ekenstam's relation [8] is recovered. Furthermore, we see that for distributions where $\bar{m}(0)$ is large, a plot of $1/\chi(r)$ against r should have gradient very close to 1.

Lastly, for the purposes of comparing theoretical predictions with experimental thermogravimetric data, we shall assume that species with fewer than m_v repeat units will be volatile gases and so the ratio of mass remaining in the distribution to initial mass $\mu(r)$ will be given by

$$\mu(r) = \frac{\sum_{m=m_v}^n m N_m(r)}{\sum_{m=1}^n m N_m(0)} = \frac{1}{\bar{m}(r)} \sum_{m=m_v}^n m f_m(r). \quad (6)$$

The final form on the RHS follows from the fact that $N_m(r) = N(r)f_m(r)$ and using Eqs. (3) and (4) to eliminate $N(r)/N(0)$.

2. Random scission

2.1. The model

Having introduced the important variables in the previous section, it is now appropriate to go on to consider a particular degradation process. In this case we shall consider the effect of random scission on the evolution of the molecular distribution, so that comparison with a polymer such as polyethylene may be made.

We shall assume that a molecule with m repeat units may undergo scission at a random bond anywhere in the molecule. For simplicity recombination will not be considered and also we shall assume that each bond is equally likely to break (these assumptions could be removed in a more sophisticated model). Thus if bond b breaks, we assume that two new molecules will be created with $m-b$ repeat units in one molecule and b repeat units in the other (see Fig. 1 for clarification).

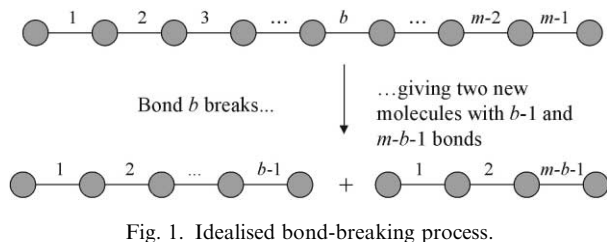


Fig. 1. Idealised bond-breaking process.

This is almost certainly a gross over-simplification of the actual bond breaking process in a polymer such as polyethylene. In the case of PE, carbon–carbon double bonds are introduced during degradation and it is unlikely that the probability of the double bond being broken is the same as a carbon–carbon single bond. Also it is unlikely that the probability of breaking a carbon–carbon single bond located in the middle of the molecule is the same as breaking a similar bond in the neighbourhood of one end of the molecule. However, in order to make progress, these complications will be ignored for the present.

Now let Δr denote an infinitesimal increment in the fraction of bonds broken. This corresponds to $\Delta r B(0)$ bonds in total. There are $N_m(r)$ molecules in the distribution with m repeat units, constituting $(m-1)N_m(r)$ bonds out of a total of $B(r)$ bonds in the whole distribution. Thus if $\Delta r B(0)$ bonds break in total, we would expect a fraction $\Delta r B(0)/B(r)$ of the $(m-1)N_m(r)$ bonds to break, so the number of bonds broken in the sample of N_m molecules will be

$$\Delta B_m = (m-1)N_m(r) \frac{B(0)}{B(r)} \Delta r = (m-1)N_m(r) \frac{\Delta r}{1-r}. \quad (7)$$

Now, assuming that one and only one bond breaks per molecule, $2\Delta B_m$ new molecules will be created with a range of repeat units uniformly distributed in the interval $[1, m-1]$. Thus the probability of a new molecule being created with j repeat units ($1 \leq j \leq m-1$) will be $1/(m-1)$ and so the expected number of new molecules with j repeat units created by the random scission of ΔB_m molecules with m repeat units will be

$$\Delta N_j(r) = 2N_m(r) \frac{\Delta r}{1-r}, \quad 1 \leq j \leq m-1. \quad (8)$$

Hence we are able to write the following balance for the new number of molecules with m repeat units:

$$N_m(r + \Delta r) = N_m(r) - (m-1)N_m(r) \frac{\Delta r}{1-r} + \frac{2\Delta r}{1-r} \sum_{j=m+1}^n N_j(r). \quad (9)$$

The second term on the RHS comes from the reduction in the number due to scission of ΔB_m molecules and the third term comes from the contribution from

scission in molecules of higher molecular weight as discussed above. Hence, as $\Delta r \rightarrow 0$, we obtain the following set of ordinary differential equations (ODEs) for the evolution of the distribution:

$$\frac{dN_m}{dr} = -\frac{(m-1)N_m}{1-r} + \frac{2}{1-r} \sum_{j=m+1}^n N_j, \quad 1 \leq m \leq n. \quad (10)$$

As a consistency check, we can use this set of ODEs to obtain an expression for the evolution of the total number of molecules $N(r)$ and compare it with the expression in the previous section $N(r) = N(0) + rB(0)$. So, on summing this set of ODEs, we obtain

$$\frac{d}{dr} \left(\sum_{m=1}^n N_m \right) = \frac{1}{1-r} \sum_{m=1}^n (m-1)N_m. \quad (11)$$

Now since $\sum_{m=1}^n (m-1)N_m$ is the number of unbroken bonds $B(r)$, we have that

$$\frac{dN}{dr} = \frac{B(r)}{1-r} = B(0), \quad (12)$$

from which the required result follows.

2.2. Exact solution for large n

For practical calculations, it is likely that n will be large and so without significant loss of generality n can be replaced by ∞ in the summation above. This simplification allows us to construct an exact solution to these equations, valid for large n . Let us look for solutions of the form $N_m(r) = Ar^s(1-r)^{m-1}$, where A and s are constants to be found. Since

$$\sum_{j=m+1}^{\infty} (1-r)^{j-1} = \frac{(1-r)^m}{r}, \quad 0 < r \leq 1, \quad (13)$$

substitution into (10) with $n = \infty$ and comparing terms shows that $s=2$. Now using the fact that $\sum_{m=1}^{\infty} N_m(r) = Ar$, $0 < r < 1$, it follows that

$$f_m(r) = r(1-r)^{m-1} \quad (14)$$

is a solution valid for large n and $0 < r \leq 1$.

Before progressing further, it is prudent to check our solution. In the light of previous attempts to model this process [8], Monte-Carlo simulations are used to calculate approximate distributions for $N_m(r)$ using an initially unimolecular distribution, i.e.

$$N_m(0) = \begin{cases} 0, & 1 \leq m < n, \\ N(0), & m = n. \end{cases} \quad (15)$$

The solution found above will not agree at $r=0$, or in the vicinity of $m=n$ when $r \sim 0$, but we expect good agreement otherwise.

In order to facilitate the comparison, a computer code was written in C using the random number generator of L'Ecuyer [14]. The standard algorithm for generating random numbers in C was not used because L'Ecuyer's method has a longer period, meaning that the algorithm may be called more times before repetition occurs.

The results in Fig. 2 were calculated using an initial distribution of 10,000 molecules with $n = 501$ [in graph

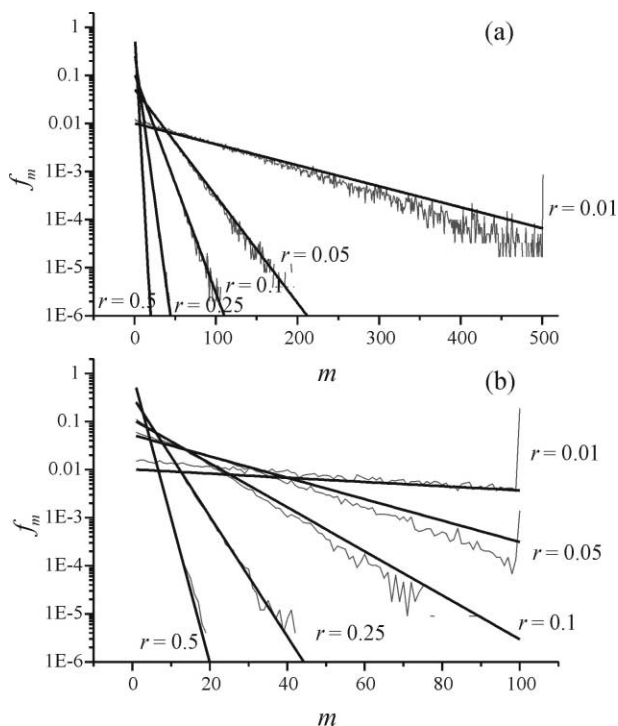


Fig. 2. Comparison of exact solution with Monte-Carlo type simulations calculated with an initial distribution of 10,000 molecules. (a) $n = 501$, (b) $n = 100$.

(a)] and $n = 100$ [in graph (b)]. In this figure, the grey curves represent the results of the Monte-Carlo simulation and the black curves represent the exact solution.

When n is not large, or the initial distribution is not unimolecular, Eq. (10) may be solved numerically using standard methods. Fig. 3 illustrates the evolution of solutions for $n = 250$ with an initially normal distribution, with average $\bar{m}(0) = 200$ and standard deviation of 50. A full discussion of the effect of initial distribution on evolution of relative frequency is beyond the scope of this work and has been discussed in the purely numerical results of Emsley and Heywood [8].

Having verified the exact solution, we now progress to an expression for $\mu(r)$, which is the main goal of this section. Given $f_m(r) = r(1-r)^{m-1}$, then

$$\bar{m}(r) = r \sum_{m=1}^{\infty} m(1-r)^{m-1} = \frac{1}{r}, \quad 0 < r \leq 1, \quad (16)$$

this following from putting $x = 1 - r$ and noting that $\sum_{m=1}^{\infty} mx^{m-1}$ is the binomial expansion for $(1-x)^{-2}$, valid for $|x| < 1$.

Also, following the reasoning above, we have that

$$\begin{aligned} \sum_{m=m_v}^{\infty} m f_m(r) &= \\ r(1-r)^{m_v-1} & \\ \left\{ m_v \sum_{j=1}^{\infty} (1-r)^{j-1} + (1-r) \sum_{j=1}^{\infty} j(1-r)^{j-1} \right\} &= \\ r(1-r)^{m_v-1} & \\ \left\{ \frac{m_v}{r} + \frac{1-r}{r^2} \right\}, & \end{aligned} \quad (17)$$

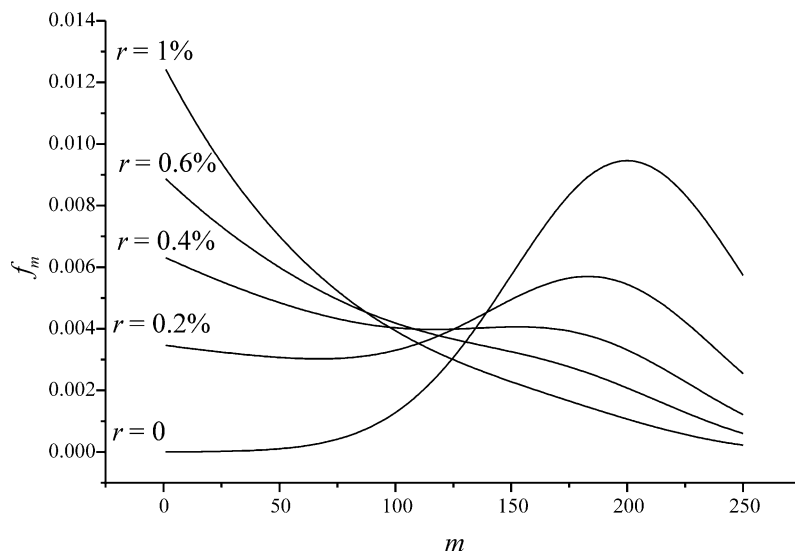


Fig. 3. Early evolution of initially normal distribution.

and so finally

$$\mu(r) = (1 - r)^{m_v - 1} \{r(m_v - 1) + 1\}. \quad (18)$$

3. Comparison with thermogravimetric experiments

3.1. Isothermal processes

In order to compare Eq. (18) with experimental data, the fraction of bonds broken r must be related to time. It seems reasonable to assume that the rate of bond breaking depends on temperature T . So, for a given linear polymer undergoing random scission, we shall assume that

$$\frac{dr}{dt} = k(T), \quad (19)$$

where k depends on the particular polymer. Furthermore, given that k now describes a temperature-dependent rate-of-bond-breaking process, it is tempting to suggest that Arrhenius temperature dependence is likely. However, it would be quite wrong to compare this bond-breaking rate $k(T)$ with the reaction rate $\kappa(T)$ used in traditional kinetic models of polymer degradation, such as in Eq. (1). In the traditional approach, κ corresponds to a global reaction rate for conversion of polymer into volatiles, or in more sophisticated multi-step schemes corresponds to a conversion rate for a particular species. Here $k(T)$ is used to describe the rate at which bonds break in the polymer molecule.

This hypothesis was investigated using a series of isothermal thermogravimetric (TG) experiments using a standard polyethylene with a number-average MW of 2015 and a reasonably narrow MW distribution (polydispersity = 1.14) supplied by Polymer Laboratories (UK) inc. (Part No. 2650-3001, batch No. 26503-1). The experiments were conducted in nitrogen using a Shimadzu TGA-50 machine. The temperature controller was programmed to increase the temperature at the machine's maximum rate of 50 K/min until the target temperature was reached.

Under isothermal conditions, dr/dt should be constant, and so one may compare a plot of $-1/\mu d\mu/dt$ vs. μ obtained from an isothermal TG experiment with a plot of $-1/\mu d\mu/dr$ vs. μ , obtained from Eq. (18) with m_v fixed at some reasonable value (recall that μ is defined as the ratio of polymer mass to initial mass). The theoretical curve is then multiplied by a factor k until it matches the experimental curve as closely as possible. In this way a graph of dr/dt vs. T may be constructed for the polymer using a series of experimental isothermal TG curves at different temperatures.

The results of this process are illustrated in Fig. 4 (a) for $m_v = 10$ and a selection of temperatures. The grey

curves correspond to isothermal TG data (smoothed using a moving average with 25 points) and the black curves correspond to curves obtained from Eq. (18) multiplied by a suitable k . The similarity between the shapes of the curves in Fig. 4(a) is striking and supports the mathematical model and the hypothesis that dr/dt is constant at constant temperature. However, the experimental data is very noisy, particularly at lower temperatures and so conclusions regarding the functional form of k should be drawn with care. Also the discrepancy at low temperatures between theory and experiment may be due to insufficient detail in the mathematical model, as discussed above in Section 3. Table 1 shows the best values of k (in a least squares sense) obtained from this procedure for $m_v = 10$ and also for $m_v = 20$ for comparison.

Also shown in Fig. 4 (b) is an Arrhenius plot of the k values for $m_v = 10$. The symbols correspond to the computed k -values, the black line is the line of best fit (in a least squares sense) and the dashed curves are the 95% confidence intervals for the line. There is increased scatter in the data at low temperatures because of the increase in noise in the TG data affecting the calculation of k . Whilst not giving conclusive proof, this figure certainly supports the possibility that k is of Arrhenius form $k(T) = A \exp(-T_A/T)$ and if we accept that this is the case, then the straight line fit gives the parameters as $A = 1.37 \times 10^{13} \text{ s}^{-1}$, $T_A = 27891 \text{ K}$ for $m_v = 10$ and $A = 1.12 \times 10^{13} \text{ s}^{-1}$, $T_A = 28156 \text{ K}$ for $m_v = 20$.

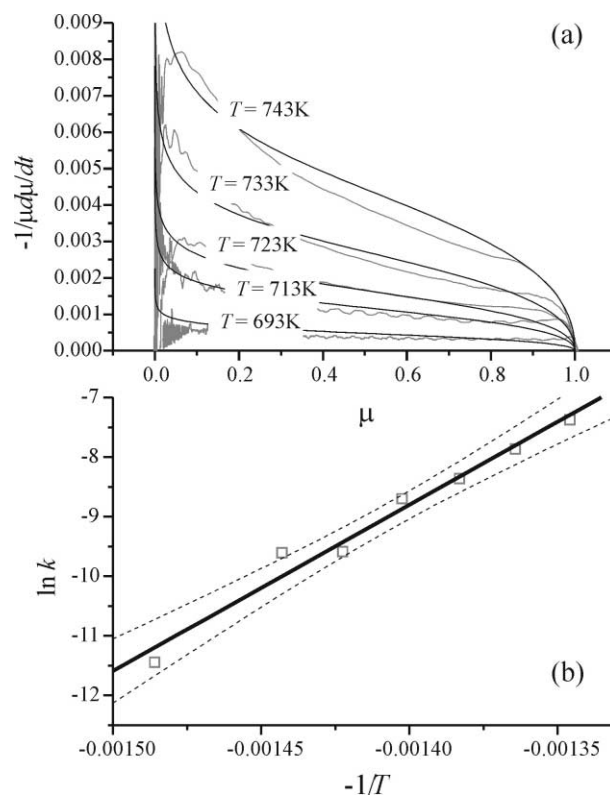


Fig. 4. Comparison with isothermal thermogravimetric data. (a) Determination of k , (b) Arrhenius plot for k .

Table 1
Results of computing $k(T) = dr/dt$ from isothermal TG data

T/K	$k (m_v = 10)/s^{-1}$	$k (m_v = 20) /s^{-1}$
673	1.07E-05	6.14E-06
693	6.76E-05	3.50E-05
703	6.88E-05	3.94E-05
713	1.67E-04	9.57E-05
723	2.34E-04	1.34E-04
733	3.84E-04	2.20E-04
743	6.27E-04	3.59E-04

As a corollary to this section, it is worth noting that for isothermal processes $r = k(T)t$ and so Ekenstam's relation (assuming that $\bar{m}(0)$ is large) takes the approximate form $1/\chi(t) - 1/\chi(0) \approx k(T)t$. Hence an analytical technique which can determine the degree of polymerisation (including degradation products) under isothermal conditions may be used as an alternative method for constructing $k(T)$.

3.2. Constant heating rate processes

In the absence of no other form for k and with the encouragement of the results from the previous section, let us assume that k is indeed of the form $k(T) = A \exp(-T_A/T)$. Given that r must be 0 when $T=0$, then for constant heating rate $dT/dt = H$, it may easily be shown that

$$r = \frac{AT}{H} e^{-T_A/T} \left\{ 1 - \frac{T_A}{T} e^{-T_A/T} E_1 \left(\frac{T_A}{T} \right) \right\}, \quad (20)$$

where E_1 is the exponential integral [15]. Furthermore, when $T_A/T \gg 1$,

$$\frac{T_A}{T} e^{-T_A/T} E_1 \left(\frac{T_A}{T} \right) \sim 1 - \frac{T}{T_A} + O \left(\frac{T}{T_A} \right)^2, \quad (21)$$

so an approximate form for r , valid for large T_A/T and more convenient for practical calculations is

$$r \approx \frac{AT^2}{HT_A} e^{-T_A/T}. \quad (22)$$

Given this final form for r , valid for constant heating rate, and the Arrhenius parameters computed in the previous section, model predictions may be compared with experimental constant heating rate TG data. The experiments were again carried out in nitrogen using a Shimadzu TGA-50 machine. Fig. 5 does precisely this for $H=10$ K/min in a nitrogen atmosphere. The grey curve corresponds to the experimental data and the black curve to the prediction from Eq. (18) with $m_v=10$, $A = 1.37 \times 10^{13} \text{ s}^{-1}$, $T_A = 27891 \text{ K}$ and r given by Eq. (22). The agreement between theory and experiment is excellent for higher temperatures (corresponding to higher times in the figure) but is not so good for lower temperatures, where errors in the Arrhenius parameters become important. However, given the arbitrary choice of m_v and the fact that the Arrhenius parameters were determined from a different set of experiments, Fig. 5 is encouraging.

If we compare this to the standard global kinetic model given by Eq. (1), then a least squares fit to the

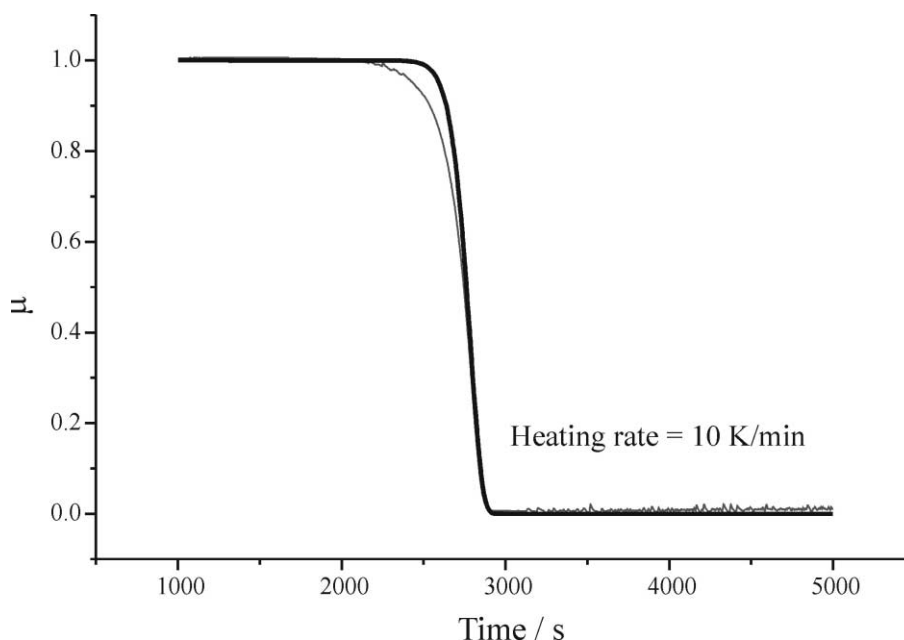


Fig. 5. Comparison between theory (thick line) and constant heating rate thermogravimetric data (thin line).

experimental data gives an activation temperature of 34,331 K, a pre-exponential factor of $5.41 \times 10^{17} \text{ s}^{-1}$ and a reaction order of 0.84.

Of course, the constant heating rate curve may be used to recalculate the Arrhenius parameters in order to provide a better fit. The advantage of using this curve is that m_v may easily become a fitting parameter, unlike in the isothermal treatment. The procedure is straightforward and is as follows:

- 1 Assume initial values for A , T_A and m_v . Then for a given heating rate H ...
- 2 For each temperature...
 - i Compute $r = \frac{AT^2}{HT_A} e^{-T_A/T}$.
 - ii Compute $\mu_{\text{theory}}(T) = (1 - r)^{m_v - 1} \{r(m_v - 1) + 1\}$.
 - iii Compute the error E between theoretical prediction and experimental value μ_{expt} : $E(T) = \{\mu_{\text{theory}}(T) - \mu_{\text{expt}}(T)\}^2$.
- 3 Compute a total residual R for the fit: $R = \int_{T_0}^{T_1} E(T) dT$, where $[T_0, T_1]$ is the temperature range of the experiment, using a suitable numerical rule, e.g. the trapezoidal rule [16].
- 3 Adjust A , T_A and m_v to give the smallest possible value for R , repeating steps 2 and 3 as necessary.

Step 4 may be accomplished using a standard minimisation algorithm. The results below were calculated using the algorithm supplied with the “Solver” add-on in MS-Excel (this is the generalised reduced gradient (GRG2) algorithm). Also, in order to give realistic

results, a constraint was placed on allowable values for m_v , namely that R be minimised subject to $5 \leq m_v \leq 20$. The best fit for the $H = 10 \text{ K/min}$ curve shown in Fig. 5 above was obtained for the parameter values $A = 3.5 \times 10^5 \text{ s}^{-1}$, $T_A = 14535 \text{ K}$, $m_v = 5$. These parameters were then used to compute theoretical curves for μ at two other heating rates (15 and 20 K/min) and the results compared with experimental curves. The results are shown in Fig. 6. The experimental curves are shown in grey and the theoretical predictions are in black. The agreement between theory and the other two experimental curves in this instance is excellent.

4. Conclusion

A simple mathematical model, intended to provide a description for the random scission of linear polymers such as polyethylene, appears to reproduce both experimental and numerical results well. Although simple in concept, the model reproduces the observed thermal degradation behaviour of a polyethylene sample (with a number-average MW of 2015 and polydispersity of 1.14) remarkably well (as determined from thermogravimetric analysis). The model also agrees with numerical Monte-Carlo type simulations.

The theoretical approach may be extended to include other important effects that have been neglected in the simple treatment above, for example recombination of molecular fragments. It may also be extended to analyse other degradation mechanisms such as end-chain scission or the combination of two scission mechanisms such as end-chain and random.

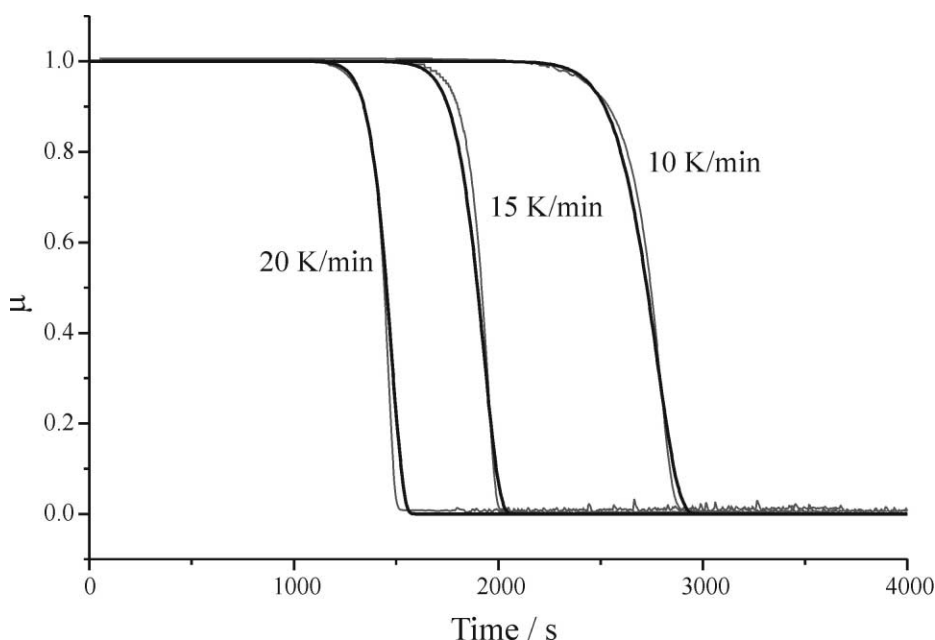


Fig. 6. Comparison between theory (thick line) and constant heating rate thermogravimetric data (thin line) at different heating rates.

Future work will include:

- further validation with other polyethylene samples,
- an investigation of other degradation mechanisms,
- application of the current model to a more complex in-depth pyrolysis model to predict ignition and heat release rate behaviour for much larger specimens.

Acknowledgements

The author would like to thank Dr S. Watt of the Australian Defence Force Academy, NSW, for some initial calculations and early discussions, and Mr S. Keith of the Department of Fuel and Energy, Leeds, for conducting the thermogravimetric experiments.

References

- [1] Cullis CF, Hirschler MM. The combustion of organic polymers. Oxford: Clarendon Press; 1981.
- [2] Staggs JEJ. Modelling thermal degradation of polymers using single-step first-order kinetics. *Fire Safety J* 1999;32:17–34.
- [3] Hatakeyama T, Quinn FX. Thermal analysis: fundamentals and applications to polymer science. Chichester: Wiley; 1994.
- [4] Frost AA, Pearson RG. Kinetics and mechanism, 2nd ed. Wiley, 1961.
- [5] Bockhorn H, Hornung A, Hornung U, Weichmann J. Kinetic study on the non-catalysed and catalysed degradation of polyamide 6 with isothermal and dynamic methods. *Thermochim Acta* 1999;337:14.
- [6] Bockhorn H, Hornung A, Hornung U, Schwaller D. Kinetic study on the thermal degradation of polypropylene and polyethylene. *J Anal Appl Pyrolysis* 1999;48:17.
- [7] Bockhorn H, Hornung A, Hornung U. Mechanisms and kinetics of thermal decomposition of plastics from isothermal and dynamic measurements. *J Anal Appl Pyrolysis* 1999;50:25.
- [8] Emsley AM, Heywood RJ. Computer modelling of the degradation of linear polymers. *Polym Degrad Stab* 1995;49:145–9.
- [9] Platowski K, Reichert K. Application of Monte Carlo methods for modelling of polymerisation reactions. *Polymer* 1999;40:1057–66.
- [10] Blastein-Barojas E, Nyden MR. Molecular dynamics study of the depolymerisation reaction in simple polymers. *Chem Phys Lett* 1990;171:499–505.
- [11] Nyden MR, Noid DW. Molecular dynamics of initial events in the thermal degradation of polymers. *J Phys Chem* 1991;95:940–5.
- [12] Nyden MR, Coley TR, Mumby S. Application of molecular dynamics to the study of thermal degradation in aromatic polymers. I: Polystyrene. *Polym Engng Sci* 1997;37:1496–500.
- [13] Doruker P, Wang Y, Mattice WL. Simulation of the random scission of C–C bonds in the initial stage of the thermal degradation of polyethylene. *Comput Theor Polym Sci* 2001;11:155–66.
- [14] L'Ecuyer P. Efficient and portable combined random number generators. *Commun ACM* 1988;31(6):742–74.
- [15] Abramowitz M, Stegun IA, editors. Handbook of mathematical functions, 9th ed. New York: Dover; 1972 [Chapter 5.1].
- [16] Press WH, Teukolsky SA, Vetterling WT, Flannery BP. Numerical recipes in C, 2nd ed. UK: Cambridge University Press; 1996 [Chapter 4.1].